Nickel−Manganese Sulfido Carbonyl Cluster Complexes. Synthesis, Structure, and Properties of the Unusual Paramagnetic Complexes Cp2Ni 2Mn(CO)3(μ3−E)2, E = S, Se

ARTICLE *in* INORGANIC CHEMISTRY · MAY 2004

Impact Factor: 4.76 · DOI: 10.1021/ic0354419 · Source: PubMed

7 AUTHORS, INCLUDING:

Richard D. Adams
Univeristy of South Caroina, Columbia, USA
685 PUBLICATIONS **10,710** CITATIONS
SEE PROFILE

Charles Edwin Webster
Mississippi State University
79 PUBLICATIONS **1,672** CITATIONS
SEE PROFILE

Josiah Manson
Texas A&M University
15 PUBLICATIONS **224** CITATIONS
SEE PROFILE

Michael B Hall
Texas A&M University
361 PUBLICATIONS **10,426** CITATIONS
SEE PROFILE

Inorg. Chem. **2004**, *43*, 2515–2525

Nickel–Manganese Sulfido Carbonyl Cluster Complexes. Synthesis, Structure, and Properties of the Unusual Paramagnetic Complexes $Cp_2Ni_2Mn(CO)_3(\mu_3\text{-}E)_2$, E = S, Se

Richard D. Adams,*,† Shaobin Miao,† Mark D. Smith,† and Horatio Farach‡

Department of Chemistry and Biochemistry and Department of Physics, University of South Carolina, Columbia, South Carolina 29208

Charles Edwin Webster, Josiah Manson, and Michael B. Hall

Department of Chemistry, Texas A&M University, College Station, Texas 77843-3255

Received December 15, 2003

The reaction of $Mn_2(CO)_7(\mu\text{-}S_2)$ with $[CpNi(CO)]_2$ yielded the paramagnetic new compound $Cp_2Ni_2Mn(CO)_3(\mu_3\text{-}S)_2$ (**1**) and a new hexanuclear metal product $Cp_2Ni_2Mn_4(CO)_{14}(\mu_6\text{-}S_2)(\mu_3\text{-}S)_2$ (**2**). Structurally, compound **1** contains two triply bridging sulfido ligands on opposite sides of an open Ni_2Mn triangular cluster. EPR and temperature-dependent magnetic susceptibility measurements of **1** show that it contains one unpaired electron. The electronic structure of **1** was determined by Fenske–Hall molecular orbital calculations which show that the unpaired electron occupies a low lying antibonding orbital delocalized unequally across the three metal atoms. The selenium homologue $Cp_2Ni_2Mn(CO)_3(\mu_3\text{-}Se)_2$ (**3**) was obtained from the reaction of a mixture of $Mn_2(CO)_{10}$ and $[CpNi(CO)]_2$ with elemental selenium and $Me_3NO{\cdot}2H_2O$. It also has one unpaired electron. Compound **1** reacted with elemental sulfur to yield the dinickeldimanganese compound, $Cp_2Ni_2Mn_2(CO)_6(\mu_4\text{-}S_2)(\mu_4\text{-}S_5)$, **4**, which can also be made from the reaction of $Mn_2(CO)_7(\mu\text{-}S_2)$ with $[CpNi(CO)]_2$ and sulfur. Compound **4** was converted back to **1** by sulfur abstraction using PPh_3. The reaction of $Mn_2(CO)_{10}$ with $[CpNi(CO)]_2$ in the presence of thiirane yielded the ethanedithiolato compound $CpNiMn(CO)_3(\mu\text{-}SCH_2CH_2S)$ (**5**), which was also obtained from the reaction of $Mn_4(CO)_{15}(\mu_3\text{-}S_2)(\mu_4\text{-}S_2)$ with $[CpNi(CO)]_2$ in the presence of thiirane. Compound **5** reacted with additional quantities of thiirane to yield the new compound $CpNiMn(CO)_3[\mu\text{-}S(CH_2CH_2S)_2]$, **6**, which contains a 3-thiapentanedithiolato ligand that bridges the two metal atoms. Compound **6** was also obtained from the reaction of $Mn_2(CO)_{10}$ with $[CpNi(CO)]_2$ and thiirane. The molecular structures of the new compounds **1**–**6** were established by single-crystal X-ray diffraction analyses.

Introduction

Transition metal complexes containing sulfido ligands present one of the most rich and varied fields of modern inorganic coordination chemistry.[1] Metal−sulfur complexes serve an important role as catalysts for the hydrodesulfurization of fossil fuels[2] and lie at the active sites in many important metalloenzymes.[3] Polynuclear metal−sulfur complexes exhibit a range of different structural types.[4] Mixed-metal sulfido cluster complexes have attracted attention because of possible synergistic effects[5] exhibited by certain types of heterogeneous metal sulfide catalysts.[6]

Insertion of a metal group into the sulfur−sulfur bond of complexes containing the disulfido ligand is a convenient route for the synthesis of heteronuclear metal complexes with sulfido ligands.[7] Recently, we have reported the new disulfido complexes $Mn_2(CO)_7(\mu\text{-}S_2)$[8] and $CpMoMn(CO)_5(\mu\text{-}S_2)$.[9] These complexes exhibit facile insertions of metal containing

* Author to whom correspondence should be addressed. E-mail: Adams@mail.chem.sc.edu.

† Department of Chemistry and Biochemistry.

‡ Department of Physics.

(1) (a) Dehnen, S.; Eichhofer, A.; Fenske, D. *Eur. J. Inorg. Chem.* **2002**, 279. (b) Shibihara, T. *Coord. Chem. Rev.* **1993**, *123*, 73. (c) Whitmire, K. H. *J. Coord. Chem.* **1988**, *17*, 95. (d) Adams, R. D.; Tasi, M. *J. Cluster Sci.* **1990**, *1*, 249. (e) Adams, R. D. *Polyhedron* **1985**, *4*, 2003.

(2) (a) Markel, E.; Van Zee, J. W. *J. Mol. Catal.* **1992**, *73*, 335. (b) Reynolds, M. A.; Guzei, I. A.; Angelici, R. J. *Organometallics* **2001**, *20*, 1071. (c) Pecararo, T. A.; Chianelli, R. R. *J. Catal.* **1981**, *83*, 430. (d) Chianelli, R. R. *Catal. Rev.* **1984**, *26*, 361. (e) Ledoux, M. J.; Michaux, O.; Agostini, G.; Panissod, P. *J. Catal.* **1986**, *102*, 275.

10.1021/ic0354419 CCC: $27.50
Published on Web 03/16/2004

fragments into the S−S bond of the disulfido ligand to yield mixed metal cluster complexes containing two triply bridging sulfido ligands, eqs 1 and 2.[7a,b,10]

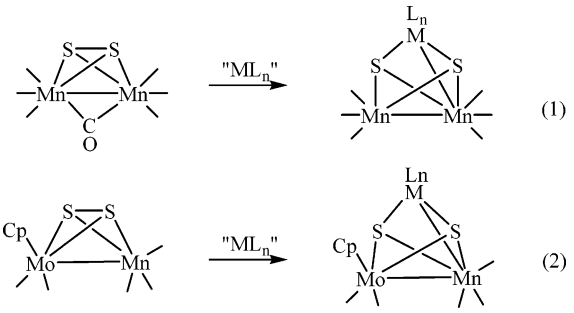

Only a few electron-deficient or electron-rich species have been reported among heteronuclear metal chalcogenide complexes.[11] We have now investigated the reaction of $Mn_2(CO)_7(\mu\text{-}S_2)$ with $[CpNi(CO)]_2$ and obtained the new complex $Cp_2Ni_2Mn(CO)_3(\mu_3\text{-}S)_2$ (**1**), which is paramagnetic with one unpaired electron. The selenium homologue $Cp_2Ni_2Mn(CO)_3(\mu_3\text{-}Se)_2$ (**3**) and several related complexes were also synthesized and fully characterized. Here we wish to report the results of our studies of compounds **1** and **3** and some of their derivatives.

Results and Discussion

The reaction of $Mn_2(CO)_7(\mu\text{-}S_2)$ with $[CpNi(CO)]_2$ yielded the new complex $Cp_2Ni_2Mn(CO)_3(\mu_3\text{-}S)_2$ **1** in 33% yield along with a minor side product $Cp_2Ni_2Mn_4(CO)_{14}(\mu_6\text{-}S_2)(\mu_3\text{-}S)_2$ **2** formed in 0.3% yield, eq 3. Complexes **1** and **2** were both fully characterized by spectroscopic methods and single-crystal X-ray diffraction analyses. The infrared spectrum of **1** exhibits three absorptions that can be attributed to the three terminal carbonyl ligands on manganese. Curiously, no resonance was observed in the ^1H NMR spectrum for the protons on the cyclopentadienyl ligands. This is attributed to the paramagnetic nature of the compound as will be described below. Details of the molecular structure of **1** were established by a single-crystal X-ray diffraction analysis.

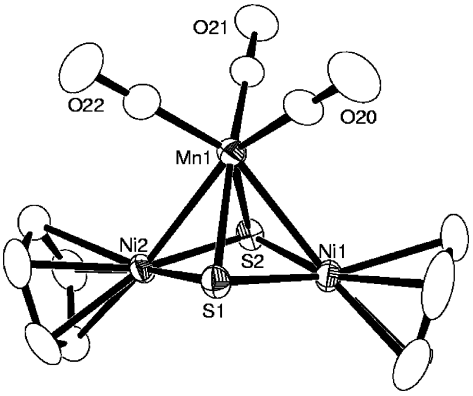

Figure 1. An ORTEP diagram of the molecular structure of $Cp_2Ni_2(\mu_3\text{-}S)_2Mn(CO)_3$, **1**, showing 40% thermal ellipsoid probability.

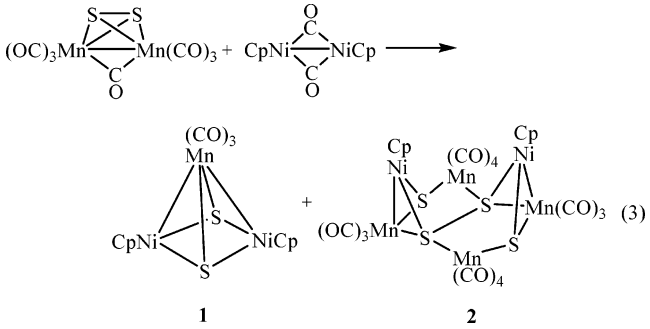

An ORTEP diagram of the molecular structure of **1** is shown in Figure 1. Selected bond distances and angles are listed in Table 1. Compound **1** contains an open triangular cluster of three metal atoms, two of nickel and one of manganese. There are only two metal−metal bonds, Mn(1)−Ni(1) = 2.5986(3) Å and Mn(1)−Ni(2) = 2.5958(3) Å. The Mn−Ni distances in **1** are shorter than that in $Cp(CO)NiMn(CO)_5$ (Mn−Ni = 2.613(1) Å),[12] which has no ligands bridging the metal−metal bond. The Ni(1)···Ni(2) distance, 3.168(1) Å, is believed to be a nonbonding interaction and is very similar to the nonbonding Ni···Ni distance, 3.145(2) Å, formulated for the structurally similar compound $[Cp_3Ni_3(\mu_3\text{-}S)_2][SbF_6]$.[13] The Mn−S bond distances, 2.2869(5) and 2.3138(5) Å, are very similar to those in $CpMoMnCpCoO(CO)_3(\mu_3\text{-}S)_2$, 2.3107(9) Å and 2.2944(8) Å.[10] The Ni−S distances (2.1595(4)−2.1672(4) Å) are longer than those in $Cp_2Ni_2Fe(CO)_3(\mu_3\text{-}S)$ (2.109(5) and 2.114(5) Å),[14] but comparable to those in $[Cp_3Ni_3(\mu_3\text{-}S)_2][SbF_6]$ (2.162(2) and 2.190(2) Å).[13]

(3) (a) Malinak, S. M.; Coucouvanis, D. *Prog. Inorg. Chem.* **2001**, *49*, 599. (b) Holm, R. H. *Pure Appl. Chem.* **1998**, *70*, 931. (c) Beinert, H.; Holm R. H.; Munck, E. *Science* **1997**, *277*, 653. (d) Holm, R. H. *Adv. Inorg. Chem.* **1992**, *38*, 1. (e) Shibahara, T. *Coord. Chem. Rev.* **1993**, *123*, 73. (f) Coucouvanis, D. *Acc. Chem. Res.* **1991**, *24*, 1. (g) Lindahl, P. A.; Kovacs, J. A. *J. Cluster Sci.* **1990**, *1*, 29. (h) Burgess, B. K. *Chem. Rev.* **1990**, *90*, 1377.

(4) (a) Wachter, J. *Angew. Chem., Int. Ed. Engl.* **1989**, *28*, 1613. (b) King, R. B.; Bitterwolf, T. E. *Coord. Chem. Rev.* **2000**, *206*−*207*, 563. (c) Whitmire, K. H. Iron Compounds without Hydrocarbon Ligands. In *Comprehensive Organometallic Chemistry II*; Wilkinson, G., Stone, F. G. A., Abel, E., Eds.; Pergamon Press: New York, 1995; Vol. 7, Chapter 1, Section 1.11.2.2, p 62 and references therein.

(5) Boudart, M.; Arrieta, J. S.; Betta, R. D. *J. Am. Chem. Soc.* **1983**, *105*, 6501 and references therein.

(6) (a) Hidai, M.; Kuwata, S.; Mizobe, Y. *Acc. Chem. Res.* **2000**, *33*, 46. (b) Casado, M. A.; Ciriano, M. A.; Edwards, A. J.; Lahoz, F. J.; Perez-Torrente, J. J.; Oro, L. A. *Organometallics* **1998**, *17*, 3414. (c) Ruffing, C. J.; Rauchfuss, T. B. *Organometallics* **1985**, *4*, 524. (d) Hobert Pawlicki, S. H.; Noll, B. C.; Rakowski DuBois, M. *J. Coord. Chem.* **2003**, *56*, 41.

(7) (a) Adams, R. D.; Kwon, O. S.; Smith, M. D. *Organometallics* **2002**, *21*, 1960. (b) Adams, R. D.; Kwon, O. S.; Smith, M. D. *Inorg. Chem.* **2002**, *41*, 1658. (c) Seyferth, D.; Henderson, R. S.; Song, L.-C. *Organometallics* **1982**, *1*, 125. (d) Don, M. J.; Richmond, M. G. *Inorg. Chim. Acta* **1993**, *210*, 129. (e) Cowie, M.; Dekock, R. L.; Wagenmaker, T. R.; Seyferth, D.; Henderson, R. S.; Gallagher, M. K. *Organometallics* **1989**, *8*, 119. (f) Day, V. W.; Lesch, D. A.; Rauchfuss, T. B. *J. Am. Chem. Soc.* **1982**, *104*, 1290. (g) Curtis, M. D.; Williams, P. D.; Butler, W. M. *Inorg. Chem.* **1988**, *27*, 2853.

(8) Adams, R. D.; Kwon, O. S.; Smith, M. D. *Inorg. Chem.* **2002**, *41*, 6281.

(9) Adams, R. D.; Captain, B.; Kwon, O. S.; Miao, S. *Inorg. Chem.* **2003**, *42*, 3356.

(10) Adams, R. D.; Miao, S. *Organometallics* **2003**, *22*, 2492.

(11) (a) Shieh, M.; Chung, R.-L.; Yu, C.-H.; Hsu, M.-H.; Ho, C.-H.; Peng, S.-M.; Liu, Y.-H. *Inorg. Chem.* **2003**, *42*, 5477. (b) Deng, Y.; Liu, Q.; Chen, C.; Wang, Y.; Cai, Y.; Wu, D.; Kang, B.; Liao, D.; Cui, J. *Polyhedron* **1997**, *16*, 4121.

(12) Madach, T.; Fischer, K.; Vahrenkamp, H. *Chem. Ber.* **1980**, *113*, 3235.

(13) North, T. E.; Thoden, J. B.; Spencer, B.; Dahl, L. F. *Organometallics* **1993**, *12*, 1299.

Table 1. Selected Intramolecular Bond Distances and Angles for **1**[a]

(a) Distances

atom	atom	distance (Å)	atom	atom	distance (Å)
Ni(1)	S(2)	2.1623(4)	Ni(2)	Mn(1)	2.5958(3)
Ni(1)	S(1)	2.1661(4)	Mn(1)	S(1)	2.2869(5)
Ni(1)	Mn(1)	2.5986(3)	Mn(1)	S(2)	2.3138(5)
Ni(2)	S(2)	2.1595(4)	C	O	1.146(2) (av)
Ni(2)	S(1)	2.1672(4)			

(b) Angles

atom	atom	atom	angle (deg)	atom	atom	atom	angle (deg)
S(2)	Ni(1)	S(1)	84.056(16)	S(1)	Mn(1)	Ni(1)	52.163(12)
S(2)	Ni(1)	Mn(1)	57.277(14)	S(2)	Mn(1)	Ni(1)	51.835(12)
S(1)	Ni(1)	Mn(1)	56.491(13)	Ni(2)	Mn(1)	Ni(1)	75.160(10)
S(2)	Ni(2)	S(1)	84.096(16)	Ni(1)	S(1)	Ni(2)	93.949(17)
S(2)	Ni(2)	Mn(1)	57.353(13)	Ni(1)	S(1)	Mn(1)	71.345(14)
S(1)	Ni(2)	Mn(1)	56.531(13)	Ni(2)	S(1)	Mn(1)	71.234(14)
S(1)	Mn(1)	S(2)	78.080(17)	Ni(2)	S(2)	Ni(1)	94.276(17)
S(1)	Mn(1)	Ni(2)	52.235(11)	Ni(2)	S(2)	Mn(1)	70.845(14)
S(2)	Mn(1)	Ni(2)	51.802(11)	Ni(1)	S(2)	Mn(1)	70.887(14)

[a] Estimated standard deviations in the least significant figure are given in parentheses.

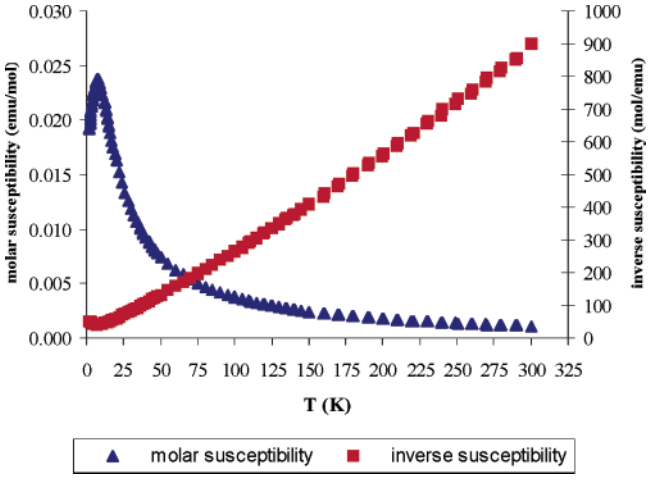

Figure 2. Molar and inverse magnetic susceptibilities of **1** as a function of temperature.

A plot of the molar magnetic susceptibility and inverse magnetic susceptibility for compound **1** in the solid state as a function of temperature is shown in Figure 2, and a plot of the effective magnetic moment as a function of temperature is shown in Figure 3. The compound exhibits normal paramagnetic behavior in the region 50−300 K. At 300 K, the effective magnetic moment, $\mu_{eff} = 1.61\ \mu_B$, is close to the spin-only value ($\mu_{eff} = 1.73\ \mu_B$) predicted for a one unpaired electron ($S = {}^1/_2$) per molecule. Below 50 K antiferromagnetic behavior sets in, indicative of intermolecular spin-coupling interactions.

Assuming that each sulfur atom serves as a 4-electron donor, compound **1** contains an odd number of electrons, a total of 51. An EPR spectrum of **1**, recorded in toluene solvent at room temperature, showed a strong resonance at $g = 2.06$ consistent with one unpaired electron. There is a small hyperfine structure of 11.5 G superimposed on the resonance due to coupling to ^{55}Mn (100% abundant, $I = {}^5/_2$);

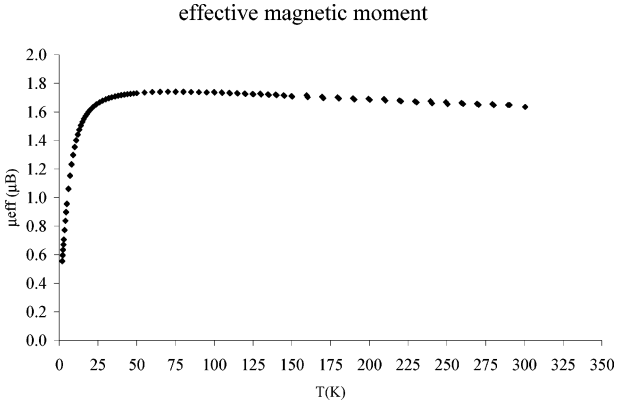

Figure 3. The effective magnetic moment of **1** in Bohr magnetons as a function of temperature.

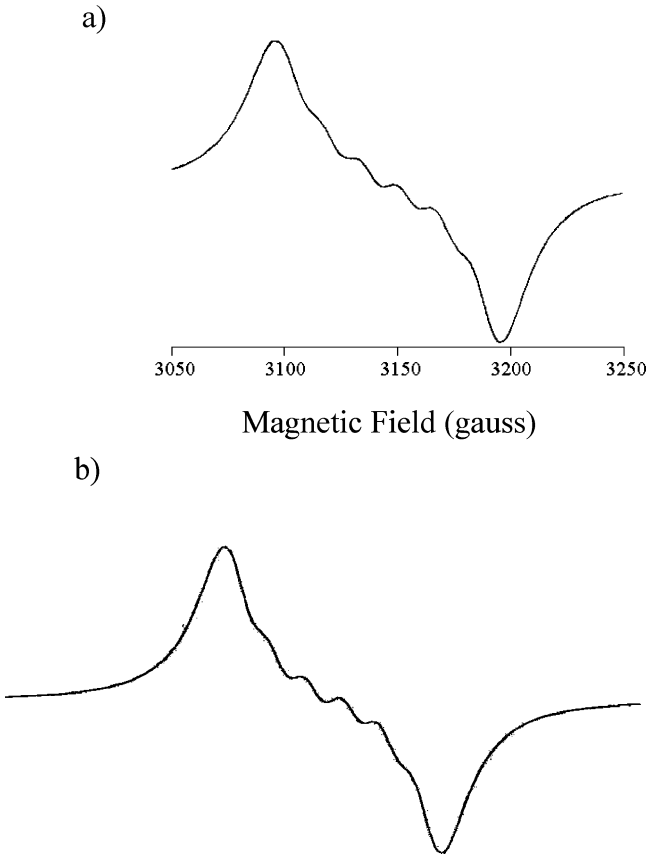

Figure 4. Experimental (a) and simulated (b) EPR spectrum of $Cp_2Ni_2(\mu_3\text{-}S)_2Mn(CO)_3$, **1**.

see Figure 4a. Manganese coupling is typically about 92 G. By using this number we can estimate that the unpaired electron populates the manganese atom approximately 13% (11.5/92) of the time; see the simulated EPR spectrum in Figure 4b.[15]

Paramagnetic trinuclear metal carbonyl cluster complexes containing nickel are not unusual.[13,14,16] The most well-known of these is the 49 electron cluster compound $Cp_3Ni_3(\mu_3\text{-}CO)_2$

(14) Braunstein, P.; Sappa, E.; Tiripicchio, A.; Tiripicchio Camellini, M. *Inorg. Chimica. Acta* **1980**, *45*, L191.

(15) *Handbook for Electron Spin Resonance*; Poole, C. P., Farach, H. A., Eds.; Springer-Verlag: New York, 1999; Vol. 2, pp 183−210.

(16) (a) Vahrenkamp, H.; Uchtman, V. A.; Dahl, L. F. *J. Am. Chem. Soc.* **1968**, *90*, 3272. (b) Maj, J. J.; Rae, A. D.; Dahl, L. F. *J. Am. Chem. Soc.* **1982**, *104*, 3054. (c) Byers, L. R.; Uchtman, V. A.; Dahl, L. F., *J. Am. Chem. Soc.* **1981**, *103*, 1942. (d) Fischer, E. O.; Palm, C. *Chem. Ber.* **1958**, *91*, 1725.

Scheme 1. An MO Correlation Diagram for **1** for Its Experimentally Determined Geometry

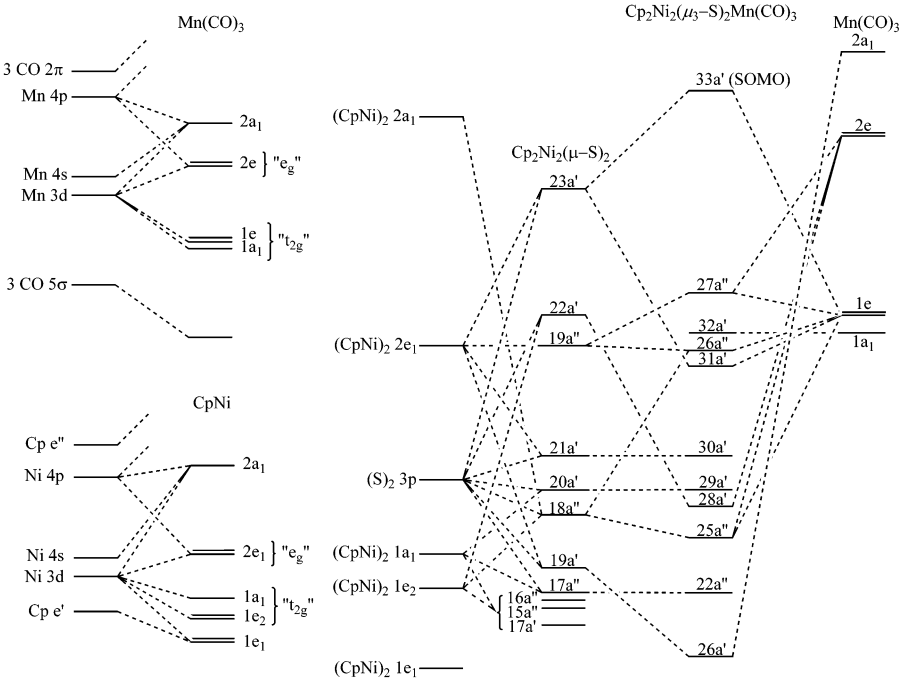

reported over 40 years ago by Fischer which has two triply bridging carbonyl ligands spanning the two triangular faces of the Ni_3 cluster.[16d] The unpaired electron in $Cp_3Ni_3(\mu_3\text{-}CO)_2$ is believed to occupy a low lying antibonding orbital delocalized across the Ni_3 cluster.[16b,c]

MO Calculations. Application of the EAN rule to **1** suggests that there should be eight 2-center, 2-electron bonds, one along each edge of the cluster, with an extra electron in an antibonding orbital. According to skeletal electron pair (SEP) counting, each CpNi contributes 3 e^-, each S contributes 4 e^-, and $Mn(CO)_3$ contributes 1 e^-. In this alternative view, this cluster has $7^1/_2$ SEPs. The correct count for a 5-vertex square pyramidal cluster is 7 SEPs for a nido cluster (octahedron missing one vertex) and 8 SEPs for an arachno cluster (pentagonal bipyramid missing two adjacent vertices). The 51 electron count for **1** is two electrons or one pair more than that of the *closo*-cluster $Cp_3Ni_3(\mu_3\text{-}CO)_2$ mentioned above, but one pair less than the count of the compound $Cp_3Ni_3(\mu_3\text{-}S)_2$ first reported by Vahrenkamp, Uchtman, and Dahl in 1968.[16a]

To develop a deeper understanding of the electronic structure of **1**, Fenske−Hall molecular orbital calculations were performed. The molecular orbital (MO) correlation diagram shown in Scheme 1 was obtained by using a suitable combination of the requisite atomic and fragment orbitals described below. The left side of Scheme 1 shows the molecular orbital structure of the two principal transition metal fragments, $Mn(CO)_3$ and CpNi. As expected for pseudo-octahedral fragments, the MO splittings show three low-lying occupied orbitals from the pseudo-octahedral "t_{2g}" set and two higher lying orbitals from the "e_g" set, which contain three electrons for CpNi and one electron for $Mn(CO)_3$. The next lowest-lying orbital for each fragment has a_1 symmetry. The right side of Scheme 1 shows the combination of two CpNi fragments with two bridging sulfurs to form the $Cp_2Ni_2(\mu\text{-}S)_2$ fragment, followed by the attachment of $Mn(CO)_3$. The key frontier orbitals of the $Cp_2Ni_2(\mu\text{-}S)_2$ fragment are pictured in Scheme 2; these representations are schematics of the principal orbital character as derived from 3-D visualizations of the MOs. In forming the $Cp_2Ni_2(\mu\text{-}S)_2$ fragment, the principal bonding interactions occur between the CpNi $2a_1$ and $2e_1$ orbitals and S 3p orbitals. The "t_{2g}" orbitals ($1e_2$ and $1a_1$) and CpNi bonding orbitals ($1e_1$) of the CpNi fragment remain occupied and essentially nonbonding in $Cp_2Ni_2(\mu_3\text{-}S)_2$ and the cluster, but they complicate the MO diagram because they occupy the same energy region as the cluster bonding pairs. The 17a′, 15a″, and 16a″ $Cp_2Ni_2S_2$ fragment orbitals correspond to the higher-lying occupied combinations of these "t_{2g}"-like orbitals and are essentially nonbonding with respect to the cluster. The four Ni−S bonding orbitals in the Ni_2S_2 "plane" are 17a″ [composed of $(CpNi)_2$ $2e_1$, $1a_1$ and S 3p], 18a″ [$(CpNi)_2$ $2a_1$, $1e_2$ and S 3p], 20a′ [$(CpNi)_2$ $2a_1$, $1a_1$, and S 3p], and 21a′ [$(CpNi)_2$ $2e_1$ and S 3p]. The remaining $Cp_2Ni_2S_2$ fragment orbitals, 19a′ [composed of $(CpNi)_2$ $2e_1$ and S 3p], 22a′ [$(CpNi)_2$ $1e_2$ and S 3p], 19a″ [$(CpNi)_2$ $2e_1$], and 23a′ [$(CpNi)_2$ $2e_1$ and S 3p], are mainly perpendicular to the Ni_2S_2 "plane".

As shown in Scheme 1, combining the frontier orbitals of $Cp_2Ni_2(\mu\text{-}S)_2$ with the frontier orbitals of $Mn(CO)_3$ (shown in Scheme 2) generates eleven high-lying orbitals for **1**; for clarity, the nonbonding "t_{2g}" orbitals of the $Cp_2Ni_2S_2$ in this energy region are not shown. Seven of these final orbitals (26a′, 22a″, 25a″, 28a′, 29a′, 30a′, and 31a′) are used for cluster bonding. Three of the seven cluster bonding orbitals, 22a″ (17a″ $Cp_2Ni_2S_2$ fragment orbital), 29a′ (20a′ $Cp_2Ni_2S_2$ fragment orbital), and 30a′ (21a′ $Cp_2Ni_2S_2$ fragment orbital), primarily contribute to cluster bonding by providing interactions between the two CpNi and two S fragments. The four remaining of these seven cluster bonding orbitals, 26a′

Scheme 2. Diagrams of Frontier Orbitals of $Cp_2Ni_2(\mu\text{-}S)_2$ and $Mn(CO)_3$

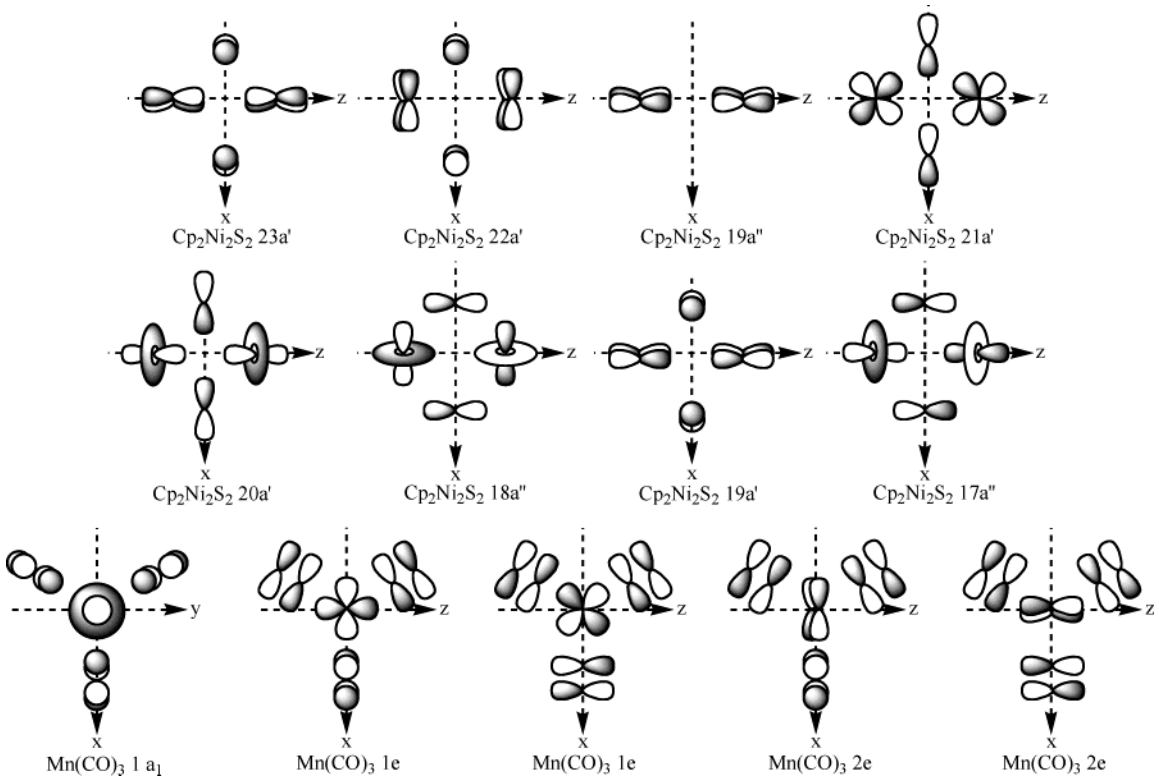

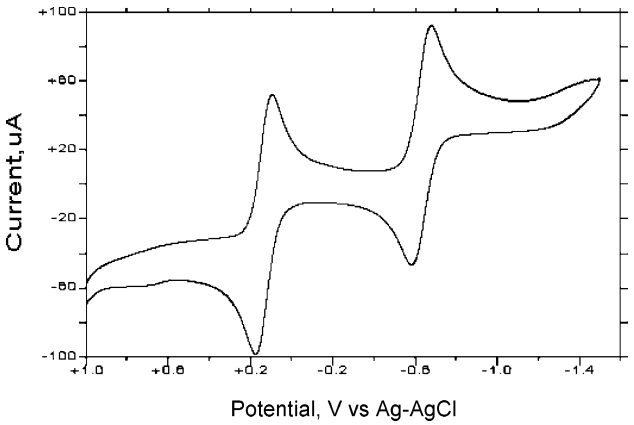

Figure 5. Cyclic voltammograms of **1**.

[composed of 19a′ $Cp_2Ni_2S_2$ and $2a_1$ $Mn(CO)_3$ fragment orbitals], 25a″ [18a″ $Cp_2Ni_2S_2$ and 2e $Mn(CO)_3$], 28a′ [22a′ $Cp_2Ni_2S_2$ and 2e $Mn(CO)_3$], and 31a′ [23a′ $Cp_2Ni_2S_2$ and 1e $Mn(CO)_3$], contribute to cluster bonding between the $Cp_2Ni_2(\mu\text{-}S)_2$ and $Mn(CO)_3$ fragments. The principal Mn−Ni bonding arises from molecular orbitals 25a″ and 31a′ shown in Figure 6. It is somewhat unexpected that one of the "t_{2g}" pairs of the $Mn(CO)_3$ fragment enters into cluster bonding, as it does in MO 31a′, by donating electron density to the empty $Cp_2Ni_2S_2$ 23a′ orbital because standard SEP counting usually does not count "t_{2g}" electron pairs from the $Mn(CO)_3$ fragment as contributors. Three of the four remaining orbitals (26a″, 32a′, and 27a″) are essentially nonbonding with respect to the $Cp_2Ni_2(\mu\text{-}S)_2$ and $Mn(CO)_3$ fragment interactions. There is a small contribution to cluster bonding from donation of electrons from the 19a″ to one of the "e_g" orbitals of the $Mn(CO)_3$ fragment in forming the cluster MO 27a″.

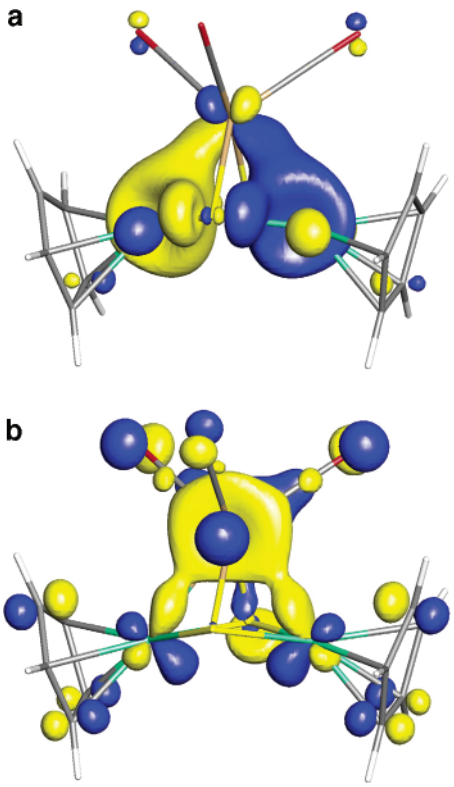

Figure 6. The two MOs containing the principal Mn−Ni bonding of **1**. Figure 6a is 25a″. Figure 6b is 31a′.

The remaining orbital, 33a′, is the singly occupied MO (SOMO, shown in Figure 7) and has antibonding character with respect to the Mn−Ni interactions, but bonding character between the Mn and the two S. The SOMO has

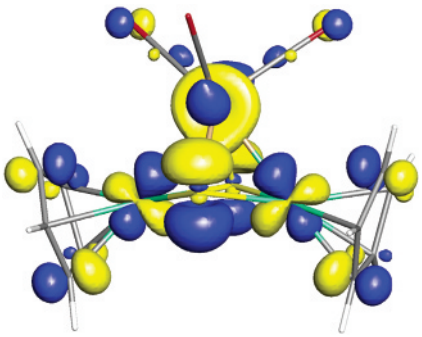

Figure 7. A diagram of the SOMO 33a′ of **1** from MO calculations.

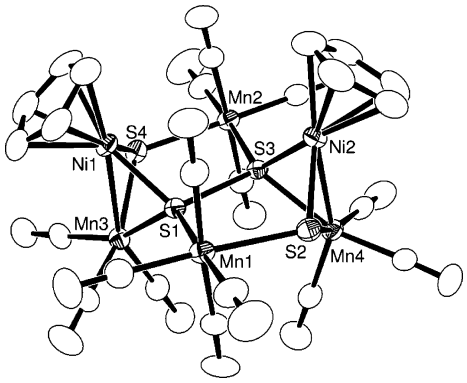

Figure 8. An ORTEP diagram of the molecular structure of $Cp_2Ni_2Mn_4(CO)_{14}(\mu_6\text{-}S_2)(\mu_3\text{-}S)_2$, **2**, showing 40% thermal ellipsoid probability.

approximately 20% Mn character, in reasonable agreement with the value derived from EPR measurements (vide supra).

Compound **1** was also studied by cyclic voltammetry (CV). A CV trace of **1** in CH_3CN solution over the range +1.00 to −1.50 V versus Ag/AgCl in CH_3CN is shown in Figure 5. Compound **1** shows one quasi-reversible one-electron reduction at $E_{1/2} = -0.631$ V, $i_{pa}/i_{pc} = 1.16$, and one reversible one-electron oxidation wave at $E_{1/2} = +0.134$ V, $i_{pa}/i_{pc} = 0.94$. These redox processes are believed to be due to the addition and removal of one electron, respectively, from the SOMO.

An ORTEP diagram of the molecular structure of **2** is shown in Figure 8. Selected bond distances and angles are listed in Table 2. Compound **2** contains six metal atoms: two of nickel and four of manganese. There are two Ni−Mn bonds, Ni(1)−Mn(3) = 2.5160(9) and Ni(2)−Mn(4) = 2.5345(8) Å; both are shorter than those in **1**. There is no bond between the two manganese atoms. The metal atoms are further linked by two triply bridging sulfido ligands, S(2) and S(4), and one μ_6-S_2 disulfido ligand, S(1)−S(3), in the center of the molecule. The S−S bond distance in the μ_6-S_2 ligand is very long, 2.2573(12) Å. Most S−S single bond distances lie in the range 1.98−2.15 Å for disulfido ligands coordinated to transition metal atoms.[17] The S−S bond distance in iron pyrite, FeS_2, which contains six iron atoms surrounding a disulfido ligand is 2.153(6) Å.[18] A longer S−S bond distance (2.297(4) Å) was observed in the compound

Table 2. Selected Intramolecular Bond Distances and Angles for **2**[a]

(a) Distances

atom	atom	distance (Å)	atom	atom	distance (Å)
Ni(1)	S(1)	2.1602(11)	Mn(3)	S(1)	2.2350(13)
Ni(1)	S(4)	2.1962(12)	Mn(3)	S(4)	2.2937(13)
Ni(1)	Mn(3)	2.5160(9)	Mn(4)	S(3)	2.2366(12)
Ni(2)	S(3)	2.1614(12)	Mn(4)	S(2)	2.2971(13)
Ni(2)	S(2)	2.1983(12)	Mn(1)	S(2)	2.3833(13)
Ni(2)	Mn(4)	2.5345(8)	S(1)	S(3)	2.2573(12)
Mn(1)	S(1)	2.3281(12)	Mn(2)	S(4)	2.3839(14)
Mn(2)	S(3)	2.3220(12)	C	O	1.131(6) (av)

(b) Angles (deg)

atom	atom	atom	angle (deg)	atom	atom	atom	angle (deg)
S(1)	Ni(1)	S(4)	87.07(4)	Ni(1)	S(1)	Mn(1)	127.16(5)
S(1)	Ni(1)	Mn(3)	56.49(3)	Mn(3)	S(1)	Mn(1)	131.74(5)
S(4)	Ni(1)	Mn(3)	57.78(3)	S(3)	S(1)	Mn(1)	105.64(5)
S(3)	Ni(2)	S(2)	87.00(5)	Ni(2)	S(2)	Mn(4)	68.60(4)
S(3)	Ni(2)	Mn(4)	56.21(3)	Ni(2)	S(2)	Mn(1)	109.46(5)
S(2)	Ni(2)	Mn(4)	57.55(4)	Mn(4)	S(2)	Mn(1)	117.30(5)
S(1)	Mn(1)	S(2)	91.13(4)	Ni(2)	S(3)	Mn(4)	70.35(4)
S(3)	Mn(2)	S(4)	90.61(4)	Ni(2)	S(3)	S(1)	107.77(5)
S(1)	Mn(3)	S(4)	82.99(5)	Mn(4)	S(3)	S(1)	110.39(5)
S(1)	Mn(3)	Ni(1)	53.69(3)	Ni(2)	S(3)	Mn(2)	126.40(5)
S(4)	Mn(3)	Ni(1)	54.10(4)	Mn(4)	S(3)	Mn(2)	130.93(5)
S(3)	Mn(4)	S(2)	82.88(4)	S(1)	S(3)	Mn(2)	106.37(5)
S(3)	Mn(4)	Ni(2)	53.43(3)	Ni(1)	S(4)	Mn(3)	68.12(4)
S(2)	Mn(4)	Ni(2)	53.86(3)	Ni(1)	S(4)	Mn(2)	108.86(6)
Ni(1)	S(1)	Mn(3)	69.82(4)	Mn(3)	S(4)	Mn(2)	118.83(5)
Ni(1)	S(1)	S(3)	106.43(5)	Mn(3)	S(1)	S(3)	111.26(5)

[a] Estimated standard deviations in the least significant figure are given in parentheses.

$[Ni_2(\mu\text{-}S_2)(cyclam)_2][ClO_4]_2$, but this disulfide ligand has a different coordination geometry.[19] Viewed as $[S_2]^{2-}$, the disulfido ligand in **2** is a 12-electron donor. All metal atoms in **2** achieve 18-electron configurations. There are various ways that one can count the electrons in **2**; one of these is represented in the structure **A**. To our knowledge, the architecture of the $Ni_2Mn_4S_4$ core observed in **2** has not been observed previously in any cluster complex.

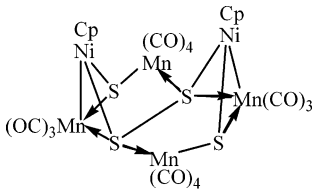

A

The selenium homologue of **1**, $Cp_2Ni_2Mn(CO)_3(\mu_3\text{-}Se)_2$ **3**, was obtained in 18% yield from the reaction of $Mn_2(CO)_{10}$ with $[CpNi(CO)]_2$ in the presence of elemental selenium, eq 4. Compound **3** has an infrared spectrum similar to that of

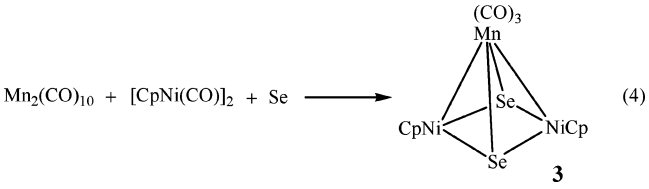

(4)

3

1, but the absorptions occur at slightly lower frequencies. An ORTEP diagram of the molecular structure of **3** is shown in Figure 9. Selected bond distances and angles are listed in

(17) Muller, A.; Jaegermann, W.; Enemark, J. H. *Coord. Chem. Rev.* **1982**, *46*, 245.
(18) Finklea, S.; Cathey, L.; Amma, E. L. *Acta Crystallogr. A* **1976**, 32, 529.
(19) Pleus, R. J.; Waden, H.; Saak, W.; Haase, D.; Pohl, S. *J. Chem. Soc., Dalton Trans.* **1999**, 2601.

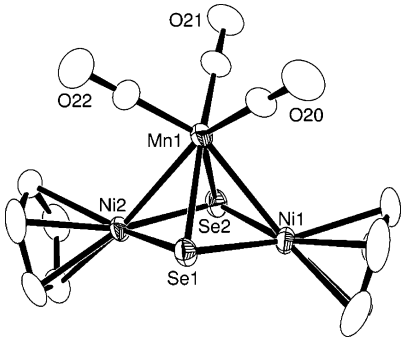

Figure 9. An ORTEP diagram of the molecular structure of $Cp_2Ni_2Mn(CO)_3(\mu_3\text{-}Se)_2$, **3**, showing 40% thermal ellipsoid probability.

Table 3. Selected Intramolecular Bond Distances and Angles for **3**[a]

(a) Distances

atom	atom	distance (Å)	atom	atom	distance (Å)
Ni(1)	Se(2)	2.2734(9)	Ni(2)	Mn(1)	2.6417(11)
Ni(1)	Se(1)	2.2751(9)	Mn(1)	Se(1)	2.4007(11)
Ni(1)	Mn(1)	2.6454(12)	Mn(1)	Se(2)	2.4336(11)
Ni(2)	Se(2)	2.2711(9)	C	O	1.145(8) (av)
Ni(2)	Se(1)	2.2827(9)			

(b) Angles

atom	atom	atom	angle (deg)	atom	atom	atom	angle (deg)
Se(2)	Ni(1)	Se(1)	84.57(3)	Se(1)	Mn(1)	Ni(1)	53.33(3)
Se(2)	Ni(1)	Mn(1)	58.73(3)	Se(2)	Mn(1)	Ni(1)	52.98(3)
Se(1)	Ni(1)	Mn(1)	57.82(3)	Ni(2)	Mn(1)	Ni(1)	78.65(3)
Se(2)	Ni(2)	Se(1)	84.45(3)	Ni(1)	Se(1)	Ni(2)	94.64(4)
Se(2)	Ni(2)	Mn(1)	58.81(3)	Ni(1)	Se(1)	Mn(1)	68.85(3)
Se(1)	Ni(2)	Mn(1)	57.80(3)	Ni(2)	Se(1)	Mn(1)	68.62(3)
Se(1)	Mn(1)	Se(2)	78.55(3)	Ni(2)	Se(2)	Ni(1)	95.00(3)
Se(1)	Mn(1)	Ni(2)	53.57(3)	Ni(2)	Se(2)	Mn(1)	68.22(3)
Se(2)	Mn(1)	Ni(2)	52.97(3)	Ni(1)	Se(2)	Mn(1)	68.29(3)

[a] Estimated standard deviations in the least significant figure are given in parentheses.

Table 3. The molecular structure of **3** is similar to that of **1**. The Mn−Ni bond distances, 2.6454(12) and 2.6417(11) Å, are longer than those in **1**. The Ni(1)···Ni(2) distance, 3.351(1) Å, is also slightly longer than that in **1** and thus is also believed to be a nonbonding interaction. The Mn−Se distances, 2.4007(11) and 2.4336(11) Å, are similar to those observed in $CpMoMn(CO)_5(\mu\text{-}Se_2)$ (2.4367(8) and 2.4218(7) Å).[20] The Ni−Se bond distances, 2.2711(9)−2.2827(9) Å, are significantly shorter than those in the compound $Cp_4Ni_4(\mu_4\text{-}Se)_2$ (2.372(1)−2.384(1) Å).[21] Like **1**, compound **3** was also expected to contain one unpaired electron, and this was confirmed by its EPR spectrum. A single resonance was observed at $g = 2.09$ with a hyperfine coupling to manganese of 15.9 G. The population of the unpaired electron on the manganese atom is approximately 17%.[15]

The compound $Cp_2Ni_2Mn_2(CO)_6(\mu_4\text{-}S_2)(\mu_4\text{-}S_5)$ (**4**) was obtained from the reaction of $Mn_2(CO)_7(\mu\text{-}S_2)$ with $[CpNi(CO)]_2$ and elemental sulfur in 10% yield, eq 5, and in an even better yield (24%) from the reaction of **1** with elemental sulfur. Compound **4** was characterized by IR, ^{1}H NMR, and single-crystal X-ray diffraction analyses. An ORTEP diagram of the molecular structure of **4** is shown in Figure 10. Selected bond distances and angles are listed in Table 4. The molecule has C_2 crystallographic symmetry. The C_2 axis passes through the atom S(4) and the center of the S(1)−S(1*) bond. The structure of **4** contains a cage of a $Ni_2Mn_2S_7$ core composed of one μ_4-disulfido ligand and one μ_4-pentasulfido ligand. The S(1)−S(1*) bond distance of 2.1061(17) Å is long, but still significantly shorter than that in **2**. There are no metal−metal bonds in the molecule. Each manganese atom is bonded to three sulfur atoms and three terminal carbonyl ligands. Each nickel atom contains one η^5-Cp ligand and two sulfur atoms. The Mn−S bond distances, 2.3014(11)−2.3563(11) Å, and the Ni−S bond

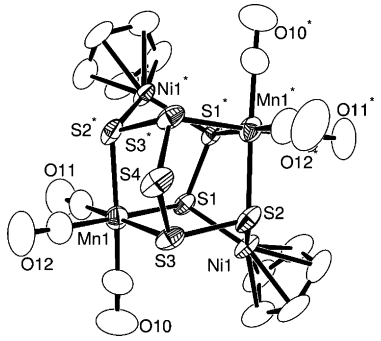

Figure 10. An ORTEP diagram of the molecular structure of $Cp_2Ni_2Mn_2(CO)_6(\mu_4\text{-}S_2)(\mu_4\text{-}S_5)$, **4**, showing 40% thermal ellipsoid probability.

Table 4. Selected Intramolecular Bond Distances and Angles for **4**[a]

(a) Distances

atom	atom	distance (Å)	atom	atom	distance (Å)
Ni(1)	S(2)	2.1599(9)	S(1)	S(1)*	2.1061(17)
Ni(1)	S(1)	2.1675(9)	S(2)	S(3)	2.1393(14)
Mn(1)	S(3)	2.3014(11)	S(3)	S(4)	2.0710(11)
Mn(1)	S(1)	2.3508(11)	C	O	1.136(6) (av)
Mn(1)	S(2)*	2.3563(11)			

(b) Angles

atom	atom	atom	angle (deg)	atom	atom	atom	angle (deg)
S(2)	Ni(1)	S(1)	93.61(3)	S(3)	S(2)	Ni(1)	99.64(5)
S(3)	Mn(1)	S(1)	90.61(4)	S(3)	S(2)	Mn(1)*	105.47(4)
S(3)	Mn(1)	S(2)*	93.03(4)	Ni(1)	S(2)	Mn(1)*	107.14(4)
S(1)	Mn(1)	S(2)*	92.22(3)	S(4)	S(3)	S(2)	99.10(5)
S(1)*	S(1)	Ni(1)	99.37(6)	S(4)	S(3)	Mn(1)	107.11(4)
S(1)*	S(1)	Mn(1)	108.20(3)	S(2)	S(3)	Mn(1)	111.46(4)
Ni(1)	S(1)	Mn(1)	109.98(4)	S(3)*	S(4)	S(3)	96.52(6)

[a] Estimated standard deviations in the least significant figure are given in parentheses.

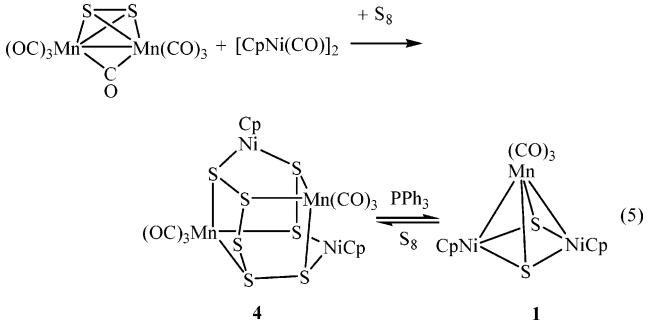

(5)

(20) Adams, R. D.; Kwon, O. S. *Inorg. Chem.* **2003** ,*42*, 6175.
(21) Fenske, D.; Hollnagel, A.; Merzweiler, K. *Angew. Chem., Int. Ed. Engl.* **1988**, *27*, 965.

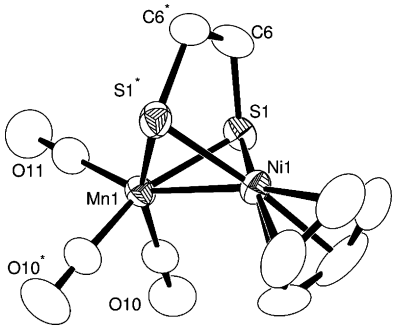

Figure 11. An ORTEP diagram of the molecular structure of CpNiMn(CO)$_3$(μ-SCH$_2$CH$_2$S), **5**, showing 40% thermal ellipsoid probability.

Table 5. Selected Intramolecular Bond Distances and Angles for **5**[a]

(a) Distances

atom	atom	distance (Å)	atom	atom	distance (Å)
Ni(1)	S(1)	2.1768(7)	S(1)	C(6)	1.823(3)
Ni(1)	Mn(1)	2.4660(7)	C(6)	C(6)*	1.498(7)
Mn(1)	S(1)	2.2696(8)	C	O	1.139(5) (av)

(b) Angles

atom	atom	atom	angle (deg)	atom	atom	atom	angle (deg)
S(1)	Ni(1)	S(1)*	84.23(4)	S(1)*	Mn(1)	Ni(1)	54.54(2)
S(1)	Ni(1)	Mn(1)	58.13(2)	C(6)	S(1)	Ni(1)	97.93(11)
S(1)	Mn(1)	S(1)*	80.06(4)	C(6)	S(1)	Mn(1)	106.61(12)
S(1)	Mn(1)	Ni(1)	54.54(2)	Ni(1)	S(1)	Mn(1)	67.33(3)
				C(6)*	C(6)	S(1)	112.96(11)

[a] Estimated standard deviations in the least significant figure are given in parentheses.

distances, 2.1599(9) and 2.1675(9) Å, are simlar to those in **1**. All metal atoms achieve 18 electron configurations. As far as we know, there are no previously reported examples of the $Ni_2Mn_2S_7$ core observed in **4**. The IR spectrum of **4** exhibits three absorptions in the carbonyl region that can be attributed to the terminal CO ligands on the Mn(CO)$_3$ groups. The ^{1}H NMR spectrum of **4** shows one singlet at 5.37 ppm that can be assigned to the equivalent Cp rings on the nickel atoms. PPh_3 reacts with **4** by extraction of five of the sulfur atoms and elimination of one of the Mn(CO)$_3$ groups to yield **1**, eq 5.

The new compound CpNiMn(CO)$_3$(μ-SCH$_2$CH$_2$S) (**5**) was obtained in 26% yield from the reaction of a mixture of Mn_4(CO)$_{15}$(μ_3-S$_2$)(μ_4-S$_2$) and [CpNi(CO)]$_2$ with thiirane. It was also obtained from the simpler reaction of $Mn_2(CO)_{10}$ and [CpNi(CO)]$_2$ with thiirane although the yield was lower, 16%. An ORTEP diagram of the molecular structure of **5** is shown in Figure 11. Selected bond distances and angles are listed in Table 5. Compound **5** contains one manganese and one nickel atom that are mutually bonded. The Ni−Mn bond distance, 2.4660(7) Å, is significantly shorter than those in **1**. There is an ethanedithiolato ligand that bridges the nickel and manganese atoms through its two sulfur atoms. The Mn−S and Ni−S bond distances 2.2696(8) and 2.1768(7) Å, respectively, are similar to those observed in **1**. In the solid state, the molecule contains a crystallographically imposed reflection plane that passes through the nickel and manganese atoms. Compound **5** is structurally similar to CpMoMn(CO)$_5$(μ-SCH$_2$CH$_2$S)[9] with a CpNi group in the place of the CpMo group. The ^{1}H NMR spectrum of **5** exhibits two multiplets due to the inequivalence of the hydrogen atoms on the methylene groups.

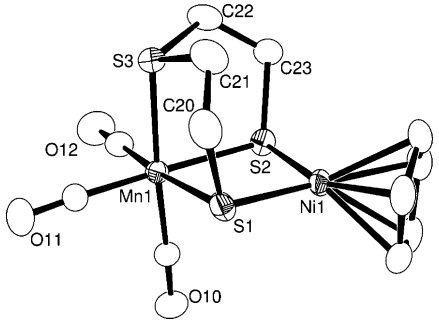

Figure 12. An ORTEP diagram of the molecular structure of **6** showing 40% thermal ellipsoid probability.

A related product, CpNiMn[μ-S(CH$_2$CH$_2$S)$_2$](CO)$_3$, **6**, was obtained in 10% yield from the same reaction by using a larger amount of thiirane. Independently, we showed that compound **6** can be obtained from directly **5** in 11% yield by reaction with thiirane, eq 6, thus **5** is probably a precursor to **6** in the first reaction. In the crystalline state, compound

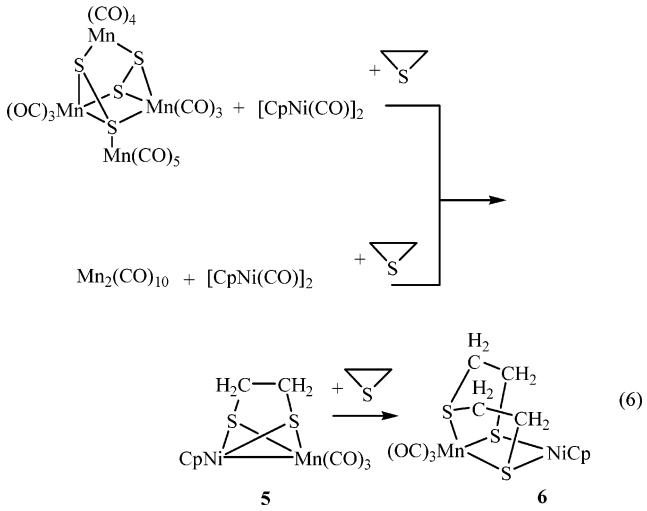

(6)

6 contains two symmetry-independent molecules in the asymmetric crystal unit. Both molecules are structurally similar, and an ORTEP diagram showing the molecular structure of one of these molecules is shown in Figure 12. Selected bond distances and angles for **6** are listed in Table 6. Each molecule contains one manganese and one nickel atom that are not mutually bonded, Mn(1)···Ni(1) = 3.290(1) Å [Mn(2)···Ni(2) = 3.287(1) Å in molecule 2]. The compound contains a 3-thiapentanedithiolato ligand that bridges the two metal atoms through the two thiolato sulfur atoms.

The Mn−S bond distances, 2.3151(10)−2.3817(10) Å, are slightly longer than those in **5**. The Ni−S bond distances, 2.1777(9)−2.1900(10) Å, are similar to those in **5**, but shorter than those in the compound [(ON)Ni(μ-S(CH$_2$)$_2$S(CH$_2$)$_2$S)-Fe(NO)$_2$] (2.2701(9)−2.2947(9) Å).[22] The thioether sulfur atom S(3) [S(6) in molecule 2] is coordinated solely to the manganese atom. This Mn−S distance, 2.3157(10) Å [2.3151-

(22) Liaw, W.-F.; Chiang, C.-Y.; Lee, G.-H.; Peng, S.-M.; Lai, C.-H.; Darensbourg, M. Y. *Inorg. Chem.* **2000**, *39*, 480.

Table 6. Selected Intramolecular Bond Distances and Angles for **6**[a]

(a) Distances

atom	atom	distance (Å)	atom	atom	distance (Å)
Ni(1)	S(1)	2.1778(10)	Mn(2)	S(5)	2.3590(10)
Ni(1)	S(2)	2.1879(10)	Mn(2)	S(4)	2.3803(9)
Ni(2)	S(5)	2.1777(9)	C(20)	C(21)	1.477(5)
Ni(2)	S(4)	2.1900(10)	C(22)	C(23)	1.490(5)
Mn(1)	S(3)	2.3157(10)	C(50)	C(51)	1.510(5)
Mn(1)	S(1)	2.3618(10)	C(52)	C(53)	1.507(5)
Mn(1)	S(2)	2.3817(10)	C	O	1.143(4) (av)
Mn(2)	S(6)	2.3151(10)	Mn(1)	Ni(1)	3.290(1)
			Mn(2)	Ni(2)	3.287(1)

(b) Angles

atom	atom	atom	angle (deg)	atom	atom	atom	angle (deg)
S(1)	Ni(1)	S(2)	91.90(4)	C(50)	S(4)	Ni(2)	104.21(12)
S(5)	Ni(2)	S(4)	91.89(3)	C(50)	S(4)	Mn(2)	105.23(12)
S(3)	Mn(1)	S(1)	87.25(4)	Ni(2)	S(4)	Mn(2)	91.89(3)
S(3)	Mn(1)	S(2)	86.19(4)	C(53)	S(5)	Ni(2)	108.47(12)
S(1)	Mn(1)	S(2)	82.83(3)	C(53)	S(5)	Mn(2)	101.06(11)
S(6)	Mn(2)	S(5)	87.60(3)	C(51)	S(6)	C(52)	101.92(17)
S(6)	Mn(2)	S(4)	86.07(3)	C(51)	S(6)	Mn(2)	103.11(12)
S(5)	Mn(2)	S(4)	82.95(3)	C(52)	S(6)	Mn(2)	105.28(12)
C(20)	S(1)	Ni(1)	106.72(13)	C(21)	C(20)	S(1)	113.5(3)
C(20)	S(1)	Mn(1)	101.83(13)	C(20)	C(21)	S(3)	110.9(3)
Ni(1)	S(1)	Mn(1)	92.80(4)	C(23)	C(22)	S(3)	114.4(3)
C(23)	S(2)	Ni(1)	103.64(13)	C(22)	C(23)	S(2)	114.9(3)
C(23)	S(2)	Mn(1)	104.52(12)	C(51)	C(50)	S(4)	114.4(2)
Ni(1)	S(2)	Mn(1)	92.01(3)	C(50)	C(51)	S(6)	114.0(2)
C(22)	S(3)	C(21)	101.2(2)	C(53)	C(52)	S(6)	110.4(2)
C(22)	S(3)	Mn(1)	102.79(14)	C(52)	C(53)	S(5)	112.7(2)
C(21)	S(3)	Mn(1)	105.32(14)				

[a] Estimated standard deviations in the least significant figure are given in parentheses.

(10) Å], is significantly shorter than the Mn−S distances to the bridging thiolato sulfur atoms. Both metal atoms have 18 electron configurations. The formation of the 3-thiapentanedithiolato ligand in the formation of **6** from **5** is clearly the result of a simple ring opening addition of thiirane to the ethandithiolato ligand in **5**. These reactions have been observed previously in reactions of thiirane with metal carbonyl complexes.[23]

To summarize, we have now prepared the new paramagnetic cluster compounds **1** and **3** that contain one unpaired electron in a low lying antibonding orbital delocalized across the metal atoms. Compound **1** reacts with elemental sulfur to yield the new cage compound **4**, which was also obtained from the reaction of $Mn_2(CO)_7(\mu\text{-}S_2)$ with $[CpNi(CO)]_2$ and sulfur. Compound **4** can be converted back to **1** by sulfur extraction when treated with PPh_3. The binuclear nickel−manganese dithiolate compounds **5** and **6** were obtained from the reaction of either $Mn_4(CO)_{15}(\mu_3\text{-}S_2)(\mu_4\text{-}S_2)$ or $Mn_2(CO)_{10}$ with $[CpNi(CO)]_2$ and thiirane. The latter was obtained from the former by a ring opening addition of thiirane to its dithiolato ligand to demonstrate still further the ability of metal complexes to oligomerize thiiranes.[24]

Experimental Section

General Data. All reactions were performed under a nitrogen atmosphere using Schlenk techniques. Reagent grade solvents were dried by the standard procedures and were freshly distilled prior to use. Infrared spectra were recorded on a Thermo-Nicolet Avatar 360 FTIR spectrophotometer. ^{1}H NMR spectra were recorded on a Varian Inova 300 spectrometer operating at 300 MHz. Mass spectra were recorded on a VG70SQ mass spectrometer. Elemental analyses were performed by Desert Analytics (Tucson, AZ). $Mn_2(CO)_{10}$ and elemental selenium were purchased from Strem Co. Ltd. $[CpNi(CO)]_2$, elemental sulfur, thiirane, and $Me_3NO{\cdot}2H_2O$ were purchased from Aldrich Co. Ltd. $Mn_2(CO)_7(\mu\text{-}S_2)$ and $Mn_4(CO)_{15}(\mu_3\text{-}S_2)(\mu_4\text{-}S_2)$ were prepared according to the published procedures.[8] Unless stated otherwise, all product separations were performed by TLC in air on Analtech 0.25 and 0.5 mm silica gel 60 Å F_{254} glass plates.

Reaction of $Mn_2(CO)_7(\mu\text{-}S_2)$ with $[CpNi(CO)]_2$. $[CpNi(CO)]_2$ (82 mg, 0.27 mmol) was added to a solution of $Mn_2(CO)_7(\mu\text{-}S_2)$ (100 mg, 0.27 mmol) in benzene (40 mL). The solution was stirred at room temperature for 24 h. The solvent was then removed in vacuo, and the residue was separated by column chromatography over silica gel by using hexane/CH_2Cl_2 (2/1, v/v) solvent mixture as eluant. $Cp_2Ni_2Mn(CO)_3(\mu_3\text{-}S)_2$, **1** (40.0 mg; 33% yield), and 1.0 mg of $Cp_2Ni_2Mn_4(CO)_{14}(\mu_6\text{-}S_2)(\mu_3\text{-}S)_2$, **2** (0.3% yield), were obtained in order of elution. Spectral data for **1**: IR ν_{CO} (cm^{-1} in hexane) 2000(vs), 1946(m), 1926(m); MS (ES) *m*/*z* 449 (M^+). Anal. Calcd: C(%), 34.64; H(%), 2.24. Found: C, 34.85; H, 2.05. Spectral data for **2**: IR ν_{CO} (cm^{-1} in CH_2Cl_2) 2090(w), 2081(m), 2019(vs), 2002(s), 1976(m), 1938(m), 1918(m); ^{1}H NMR (δ in $CDCl_3$) 5.55 (s, 10H).

Synthesis of 3. $[CpNi(CO)]_2$ (82 mg, 0.27 mmol) was added to a solution of $Mn_2(CO)_{10}$ (100 mg, 0.26 mmol), $Me_3NO{\cdot}2H_2O$ (85 mg, 0.76 mmol), and elemental selenium (100 mg, 1.27 mmol) in CH_2Cl_2 (30 mL). The mixture was stirred at room temperature for 24 h. The solvent was removed in vacuo, and the residue was separated by column chromatography over silica gel by using a hexane/CH_2Cl_2 (2/1, v/v) solvent mixture as eluant. $Cp_2Ni_2Mn(CO)_3(\mu_3\text{-}Se)_2$, **3** (25 mg; 18% yield), was obtained. Spectral data for **3**: IR ν_{CO} (cm^{-1} in hexane) 1994(vs), 1937(m), 1920(m); MS (ES) *m*/*z* 545 (M^+).

Synthesis of 4. $[CpNi(CO)]_2$ (82 mg, 0.27 mmol) was added to a solution of $Mn_2(CO)_7(\mu\text{-}S_2)$ (100 mg, 0.27 mmol), $Me_3NO{\cdot}2H_2O$ (60 mg, 0.54 mmol), and elemental sulfur (87 mg, 2.7 mmol) in CH_2Cl_2 (30 mL). The mixture was stirred at room temperature for 24 h. The solvent was then removed in vacuo, and the residue was separated by TLC by using a hexane/CH_2Cl_2 (3/1, v/v) solvent mixture as eluant. $Cp_2Ni_2Mn_2(CO)_6(\mu_4\text{-}S_2)(\mu_4\text{-}S_5)$, **4** (20.0 mg; 10% yield), was obtained. Spectral data for **4**: IR ν_{CO} (cm^{-1} in hexane) 2023(vs), 1968(s), 1956(s); ^{1}H NMR (δ in $CDCl_3$) 5.37 (s, 10H). Anal. Calcd: C(%), 25.62; H(%), 1.34. Found: C, 25.91; H, 1.33.

Synthesis of 5. Method 1. $[CpNi(CO)]_2$ (54 mg, 0.18 mmol) was added to a solution of $Mn_2(CO)_{10}$ (70 mg, 0.18 mmol), $Me_3NO{\cdot}2H_2O$ (30 mg, 0.27 mmol), and thiirane (22 μL, 0.37 mmol) in CH_2Cl_2 (30 mL). The mixture was stirred at room temperature for 24 h. The solvent was then removed in vacuo, and the residue was separated by TLC by using a hexane/CH_2Cl_2 (3/1, v/v) solvent mixture as eluant. $CpNiMn(\mu\text{-}SCH_2CH_2S)(CO)_3$, **5** (10 mg; 16% yield), was obtained. Spectral data for **5**: IR ν_{CO} (cm^{-1} in hexane) 2010(vs), 1932(s), 1925(s); ^{1}H NMR (δ in $CDCl_3$) 5.44 (s, 5H), 2.78−2.73 (q, 2H), 1.96−1.92 (q, 2H). Anal. Calcd: C(%), 33.84; H(%), 2.56. Found: C, 33.63; H, 2.68.

Method 2. $[CpNi(CO)]_2$ (10.0 mg, 0.033 mmol) was added to a solution of $Mn_4(CO)_{15}(\mu_3\text{-}S_2)(\mu_4\text{-}S_2)$ (25 mg, 0.033 mmol) and thiirane (5 μL, 0.083 mmol) in 30 mL of CH_2Cl_2. The mixture was stirred at room temperature for 24 h in the presence of irradiation from a 60-W visible lamp placed 10 cm from the reaction

(23) Adams, R. D.; Chen, G.; Sun, S.; Wolfe, T. A. *J. Am. Chem. Soc.* **1990**, *112*, 868.
(24) Adams, R. D. *Acc. Chem. Res.* **2000**, *33*, 171.

flask. The solvent was then removed in vacuo, and the residue was separated by TLC by using a hexane/CH_2Cl_2 (3/1, v/v) solvent mixture as eluant; 3.0 mg of **5** (26% yield) was obtained.

Synthesis of 6. $[CpNi(CO)]_2$ (23.0 mg, 0.076 mmol) was added to a solution of $Mn_2(CO)_{10}$ (30 mg, 0.077 mmol), $Me_3NO{\cdot}2H_2O$ (30 mg, 0.27 mmol), and thiirane (0.15 mL, 2.5 mmol) in CH_2Cl_2 (30 mL). The mixture was stirred at room temperature for 20 h. The solvent was removed in vacuo, and the residue was separated by TLC by using a hexane/CH_2Cl_2 (3/1, v/v) solvent mixture as eluant. $CpNiMn[\mu\text{-}S(CH_2CH_2S)_2](CO)_3$, **6** (3.2 mg; 10% yield), was obtained. Spectral data for **6**: IR ν_{CO} (cm^{-1} in hexane) 2025(vs), 1947(s), 1926(s); ^1H NMR (δ in $CDCl_3$) 5.01 (s, 5H), 4.08−4.01 (m, 2H), 3.45−3.39 (m, 2H), 2.55−2.46 (m, 2H), 1.81−1.72 (m, 2H). Anal. Calcd: C(%), 34.72; H(%), 3.16. Found: C, 34.77; H, 3.23.

Reaction of 1 with Elemental Sulfur. Elemental sulfur (7.0 mg, 0.22 mmol) was added to a solution of **1** (10 mg, 0.022 mmol) in benzene (30 mL). The mixture was heated to reflux for 12 h. The solvent was then removed in vacuo, and the residue was separated by TLC by using a hexane/CH_2Cl_2 (3/1, v/v) solvent mixture as eluant; 4.0 mg of **4** (24% yield) was obtained.

Reaction 4 with Ph_3P. Ph_3P (34.0 mg; 0.13 mmol) was added to a solution of **4** (10.0 mg, 0.013 mmol) in 30 mL of benzene. The mixture was stirred at room temperature for 8 h. The solvent was then removed in vacuo, and the residue was separated by column chromatography over silica gel by using a hexane/CH_2Cl_2 (6/1, v/v) solvent mixture as eluant; 1.1 mg of **1** (18% yield) was obtained.

Transformation of 5 to 6. Thiirane (3.0 μL; 0.050 mmol) was added to a solution of **5** (8.0 mg, 0.023 mmol) and $Me_3NO{\cdot}2H_2O$ (4.2 mg, 0.038 mmol) in 20 mL of CH_2Cl_2. The mixture was heated to reflux for 8 h. The solvent was then removed in vacuo, and the residue was separated by TLC using a hexane/CH_2Cl_2 (3/1, v/v) solvent mixture as eluant; 1.0 mg of **6** (11% yield) was obtained.

EPR Measurements and Spectral Simulations. Electron paramagnetic resonance spectra were measured at an X band Varian instrument. For **1**: center field 3150 G, sweep 200 G, gain 80 × 10, modulation 0.5 G, time constant 0.128 s, Δg 0.04, g 2.06, line width 14.6 G, hyperfine constant 11.5 G. For **3**: center field 3100 G, sweep 500 G, gain 3.2 × 1000 × 10, modulation 0.25 G, time constant 0.5 s, Δg 0.07, g 2.09, line width 30.0 G, hyperfine constant 15.9 G. The room temperature solution spectra were recorded in benzene. Simulations of the EPR spectra were performed by using a locally written program by H. Farach. The sample was calibrated by using DPPH, diphenylpicrylhydrazyl.

Electrochemical Measurements. Cyclic voltammetric experiments were conducted by using a CV-50W voltammetric analyzer purchased from Bioanalytical Systems, West Lafayette, IN. The experiments were done under nitrogen at ambient temperature in solutions with 0.1 mol/L tetrabutylammonium hexafluorophosphate as the supporting electrolyte. Cyclic voltammograms (CVs) were obtained by using a three-electrode system consisting of a platinum working electrode, a platinum counter, and a Ag/AgCl reference electrode using a sweep rate of 200 mV/s. Half-wave potentials ($E_{1/2}$) were calculated as the mean potential between the peak potential by use of the equation $E_{1/2} = (E_{pa} + E_{pc})/2$, where E_{pa} is the anodic peak potential and E_{pc} is the cathodic peak potential. Two redox events were observed for compound **1**: a one electron reduction at −631 mV with $E_{pa} - E_{pc} = 94$ mV and $i_{pa}/i_{pc} = 1.16$ and a one electron oxidation at 135 mV with $E_{pa} - E_{pc} = 79$ mV and $i_{pa}/i_{pc} = 0.94$.

Magnetic Measurements. Magnetic susceptibility of $Cp_2Ni_2Mn(\mu_3\text{-}S)_2(CO)_3$ was measured using a Quantum Design MPMS XL SQUID magnetometer, at an applied field strength of 5 kG. Both field cooled (fc) and zero-field cooled (zfc) measurements were performed in the temperature range 2−300 K. The sample was contained in a gelatin capsule fastened in a plastic straw for immersion into the SQUID. The very small diamagnetic contribution of the gelatin capsule containing the sample had a negligible contribution to the overall magnetization.

Table 7. Crystallographic Data for Compounds **1** and **2**

compound	**1**	**2**
empirical formula	$C_{13}H_{10}MnNi_2O_3S_2$	$C_{24}H_{10}Mn_4Ni_2O_{14}S_4{\cdot}CH_2Cl_2$
fw	450.69	1072.67
crystal system	monoclinic	monoclinic
space group	$P2_1/c$	Pn
a (Å)	7.9856(4)	12.2178(8)
b (Å)	10.5400(5)	10.1080(7)
c (Å)	18.1775(8)	14.5679(10)
α (deg)	90	90
β (deg)	99.684(1)	95.280(1)
γ (deg)	90	90
V (Å^3)	1508.17(12)	1791.5(2)
Z	4	2
temperature (K)	296(2)	296(2)
ρ_{calc} (g/cm^3)	1.985	1.989
μ (Mo Kα) (mm^{-1})	3.574	2.842
no. of observations ($I > 2\sigma(I)$)	3404	6169
no. of parameters	230	460
GOF[a]	1.080	1.036
max shift in final cycle	0.001	0.001
residuals: R1; wR2 [b]	0.0233; 0.0573	0.0349; 0.0744
absorption correction, max/min	SADABS, 1.0000/0.674	SADABS, 1.000/0.702
largest peak in diff map (e$^-$/Å^3)	0.324	0.626

[a] $GOF = [\sum_{hkl}(w(|F_{obs}^2| - |F_{calc}^2|))^2/(n_{data} - n_{vari})]^{1/2}$. [b] $R1 = \sum(||F_{obs}| - |F_{calc}||)/\sum|F_{obs}|$. $wR2 = \{\sum[w(|F_{obs}^2 - F_{calc}^2|)^2/\sum[w(F_{obs}^2)^2]\}^{1/2}$; $w = 1/\sigma^2(F_{obs}^2)$.

Crystallographic Analysis. Dark-red crystals of **1**, **2**, **4**, and **5** and brown-green crystals of **6** were grown by slow evaporation of solvent from solutions of the complex in hexane/methylene chloride solvent mixtures at 4 °C. Dark-red single crystals of **3** suitable for diffraction analysis were grown by slow evaporation of solvent from a hexane solution at −20 °C. The data crystal of each compound was mounted by gluing onto the end of a thin glass fiber. X-ray intensity data were measured by using a Bruker SMART APEX CCD-based diffractometer by using Mo Kα radiation ($\lambda = 0.71073$ Å). All unit cells were initially determined on the basis of reflections selected from a set of three scans measured in orthogonal wedges of reciprocal space. The raw data frames were integrated with the SAINT+ program using a narrow-frame integration algorithm.[25] Corrections for the Lorentz and polarization effects were also applied by using the program SAINT. An empirical absorption correction based on the multiple measurement of equivalent reflections was applied for each analysis by using the program SADABS. Crystal data, data collection parameters, and results of the analyses for compounds **1**−**6** are listed in Tables 7−9. All structures were solved by a combination of direct methods and difference Fourier syntheses. All non-hydrogen atoms were refined with anisotropic thermal parameters. The positions of the hydrogen atoms were calculated by assuming idealized geometries and were refined by using the riding model. Refinements were carried out on F^2 by the method of full-matrix least squares by using the SHELXTL program library with neutral atom scattering factors.[26]

(25) *SAINT+*, version 6.02a; Bruker Analytical X-ray Systems, Inc.: Madison, WI, 1998.

Table 8. Crystallographic Data for Compounds **3** and **4**

compound	**3**	**4**
empirical formula	$C_{13}H_{10}MnNi_2O_3Se_2$	$C_{16}H_{10}Mn_2Ni_2O_6S_7$
fw	544.49	749.96
crystal system	monoclinic	orthorhombic
space group	$P2_1/c$	$Ccc2$
a (Å)	7.9474(7)	16.7406(11)
b (Å)	10.6804(10)	19.2196(12)
c (Å)	18.4082(17)	7.8675(5)
α (deg)	90	90
β (deg)	98.694(2)	90
γ (deg)	90	90
V (Å^3)	1544.6(2)	2531.3(3)
Z	4	4
temperature (K)	296(2)	296(2)
ρ_{calc} (g/cm^3)	2.342	1.968
μ (Mo Kα) (mm^{-1})	7.933	3.048
no. of observations ($I > 2\sigma(I)$)	2910	2836
no. of parameters	230	170
GOF[a]	0.985	1.040
max shift in final cycle	0.001	0.002
residuals: R1; wR2[b]	0.0529; 0.1347	0.0316; 0.0638
absorption correction, max/min	SADABS, 1.000/0.651	SADABS, 1.000/0.734
largest peak in diff map (e$^-$/Å^3)	1.149	0.405

[a] GOF = $[\sum_{hkl}(w(|F_{obs}^2| - |F_{calc}^2|))^2/(n_{data} - n_{vari})]^{1/2}$. [b] R1 = $\sum(||F_{obs}| - |F_{calc}||)/\sum|F_{obs}|$. wR2 = $\{\sum[w(|F_{obs}^2 - F_{calc}^2|)^2/\sum[w(F_{obs}^2)^2]\}^{1/2}$; $w = 1/\sigma^2(F_{obs}^2)$.

Table 9. Crystallographic Data for Compounds **5** and **6**

compound	**5**	**6**
empirical formula	$C_{10}H_9MnNiO_3S_2$	$C_{12}H_{13}MnNiO_3S_3$
fw	354.94	415.05
crystal system	orthorhombic	triclinic
space group	$Pnma$	$P\bar{1}$
a (Å)	12.2308(10)	9.3111(5)
b (Å)	10.5483(10)	11.8280(6)
c (Å)	10.3020(10)	14.8528(8)
α (deg)	90	105.764(1)
β (deg)	90	93.297(1)
γ (deg)	90	90.003(1)
V (Å^3)	1329.1(2)	1571.43(14)
Z	4	4
temperature (K)	293(2)	293(2)
ρ_{calc} (g/cm^3)	1.774	1.754
μ (Mo Kα) (mm^{-1})	2.67	2.40
no. of observations ($I > 2\sigma(I)$)	1567	6250
no. of parameters	85	361
GOF[a]	1.063	1.048
max shift in final cycle	0.000	0.001
residuals: R1; wR2[b]	0.0359; 0.0820	0.0504; 0.1057
absorption correction, max/min	SADABS, 1.000/0.897	SADABS, 1.0000/0.824
largest peak in diff map (e$^-$/Å^3)	0.479	0.737

[a] GOF = $[\sum_{hkl}(w(|F_{obs}^2| - |F_{calc}^2|))^2/(n_{data} - n_{vari})]^{1/2}$. [b] R1 = $\sum(||F_{obs}| - |F_{calc}||)/\sum|F_{obs}|$. wR2 = $\{\sum[w(|F_{obs}^2 - F_{calc}^2|)^2/\sum[w(F_{obs}^2)^2]\}^{1/2}$; $w = 1/\sigma^2(F_{obs}^2)$.

Compounds **1** and **3** both crystallized in the monoclinic crystal system. They are isomorphous. The space group $P2_1/c$ was uniquely identified on the basis of the systematic absences observed in the data. All non-hydrogen atoms were refined with anisotropic thermal parameters.

Compound **2** crystallized in the monoclinic crystal system. The systematic absences in the data were consistent with either of the space groups $P2/n$ and Pn. The noncentric space group Pn was selected and confirmed by the successful solution and refinement of the structure. One equivalent of CH_2Cl_2 from the crystallization solvent was found cocrystallized with the complex in the asymmetric unit of the unit cell.

Compound **4** crystallized in the orthorhombic crystal system. The systematic absences in the data were consistent with the space groups $Cccm$ and $Ccc2$. The noncentric space group $Ccc2$ was assumed and confirmed by the successful solution and refinement of the structure. In the solid state the molecule possesses a crystallographically imposed C_2 symmetry.

Compound **5** crystallized in the orthorhombic crystal system. The systematic absences in the data were consistent with either of the space groups $Pnma$ and $Pna2_1$. The centric space group $Pnma$ was tested first and confirmed by the successful solution and refinement of the structure. In the solid state the molecule possesses a crystallographically imposed reflection symmetry.

The compound **6** crystallized in the triclinic crystal system. The centrosymmetric space group $P\bar{1}$ was assumed and confirmed by the successful solution and refinement of the structure. All non-hydrogen atoms were refined with anisotropic thermal parameters.

Molecular Orbital Calculations. The Fenske−Hall[27] calculations of **1** were performed utilizing a graphical user interface developed[28] to build inputs for and view outputs from stand-alone Fenkse−Hall (version 5.2) and MOPLOT2[29] binary executables. Contracted double-ζ basis sets were used for the Ni and Mn 4d, S 3p, and C and O 2p atomic orbitals.

Acknowledgment. This research was supported by a grant from the National Science Foundation, Grants CHE-9909017 and CHE-9800184, and the Welch Foundation (A-648). We thank Mr. Matthew Davis for making the magnetic susceptibility measurements. Partial support of this research was provided by the USC NanoCenter.

Supporting Information Available: Molecular orbital depictions and crystallographic data in CIF format. This material is available free of charge via the Internet at http://pubs.acs.org.

IC0354419

(26) Sheldrick, G. M. *SHELXTL*, version 5.1; Bruker Analytical X-ray Systems, Inc.: Madison, WI, 1997.

(27) Hall, M. B.; Fenske, R. F. *Inorg. Chem.* **1972**, *11*, 768.

(28) Manson, J.; Webster, C. E.; Hall, M. B. JIMP Development Version 0.1 (built for Windows PC and Redhat Linux); Department of Chemistry, Texas A&M University, College Station, TX 77842 (http://www.chem.tamu.edu/jimp/) (accessed May 2003).

(29) MOPLOT2: for orbital and density plots from linear combinations of Slater or Gaussian type orbitals; Version 2.0, June 1993; Dennis L. Lichtenberger, Department of Chemistry, University of Arizona, Tucson, AZ 85721.